Localization of a FITC-Labeled Phosphorothioate Oligodeoxynucleotide in the Skin After Topical Delivery by Iontophoresis and Electroporation

Vincent Regnier[1] and Véronique Préat[1,2]

Received April 23, 1998; accepted July 17, 1998

Purpose. The aim of this study was to verify the hypothesis that the application of high voltage to the skin enhances both stratum corneum and keratinocyte permeability. Therefore, the transport of FITC labelled phosphorothioate oligonucleotides (FITC-PS) administered by passive diffusion, iontophoresis or electroporation was localized.

Methods. Fluorescent microscopy and laser scanning confocal microscopy were used to visualize the FITC-PS transport at the tissue and cell level respectively in hairless rat skin after electroporation (5 × (200 V ~ 500 ms) or iontophoresis (same amount of charges transferred).

Results. FITC-PS did not penetrate the viable skin by passive diffusion. Molecular transport in the skin upon electroporation or iontophoresis was localized and implied mainly hair follicles for iontophoresis. In the stratum corneum, the pathways for FITC-PS transport were more transcellular during electroporation and paracellular during iontophoresis. FITC-PS were detected in the nucleus of the keratinocytes a few minutes after pulsing. In contrast, iontophoresis did not lead to an uptake of the oligomer.

Conclusions. The internalization of FITC-PS in the keratinocytes after electroporation confirms the hypothesis and suggests that electroporation, which allows both efficient topical delivery and rapid cellular uptake of the oligonucleotides, might be useful for antisense therapy of epidermal diseases.

KEY WORDS: electroporation; iontophoresis; oligonucleotides; localization; topical delivery; transdermal delivery; skin.

INTRODUCTION

Antisense oligonucleotide (ON) technology uses single-stranded DNA to modulate the transfer of information from gene to protein. This property has made ON a potentially useful tool in dissecting gene function in cells in culture and in inhibiting genes causing diseases. Many methods have been proposed to increase ON delivery to the target cells, to increase their resistance to nucleases and/or to enhance their cellular uptake (1–4).

The accessibility of the skin makes it an easy target for topical antisense therapy. A wide variety of skin diseases are potential candidates for antisense therapy by topical delivery. However, ON transdermal delivery is limited by the low permeability of the skin (5). Therefore, delivery methods other than passive permeation have been investigated.

High intensity electric field pulses can temporarily destabilize and permeabilize lipid bilayers. This universal phenomenon, called electroporation or electropermeabilization (6), is a commonly used method for introducing DNA into isolated cells. More recently, electroporation has been shown to increase transdermal drug delivery by transient permeabilization of the multiple lipid bilayers of the stratum corneum, the rate limiting barrier of the skin (7–10). We have recently shown that electroporation also enhances the topical delivery of ON (11). Therapeutic levels of an intact phosphorothioate ON (PS) were reached in the viable tissues of hairless rat skin *in vitro* within a few minutes (12). PS level in the target tissue could be controlled (11). PS was mainly transported in the targeted tissue by electrophoresis through a permeabilized skin. The drug reservoir created during pulsing remained for more than 4 hours (12).

In addition to its potency to deliver ON (11–13), electroporation might also facilitate ON uptake by skin cells. Indeed, electroporation is able to permeabilize skin cells *in vivo*, as assessed by electrochemotherapy (electroloading of bleomycin in tumoral cells (14)), or by the efficient transfection of mouse skin cells by plasmid DNA (15–16). Moreover, the rapid electroloading of ON into the target cells could improve their potency (17).

Iontophoresis (i.e., the permeation of ionized or neutral molecules across biological membranes under the influence of electrical current) has also been shown to enhance ON across hairless skin *in vitro* (18–19). However, in contrast to electroporation, iontophoresis is not believed to permeate the cells of the treated tissue. Iontophoresis acts more on the drug than on the skin structures, electrophoresis being the main driving force for transdermal delivery of ON (7,18). We recently found that both iontophoresis and electroporation of same amount of charges transferred (Q) were efficient to deliver a phosphorothioate ON (PS) topically (12). However, since besides enhancing skin permeability and providing a driving force, electroporation could also permeabilize the epidermal cells, electroporation could be more interesting than iontophoresis to deliver topically ON in the skin.

The aim of this study was to check the hypothesis that electroporation enhances both stratum corneum and corneocyte permeability. Therefore, the routes of passage and the distribution of the antisense ON within the skin at the tissular and cellular level were studied after ON delivery after passive diffusion, iontophoresis and electroporation.

MATERIAL AND METHODS

Oligonucleotides

The oligonucleotide used (PS) (Eurogentec, Seraing, Belgium) had all internucleoside links of phosphorothioate type. Its sequence (5′ ACC AAT CAG ACA CCA 3′) is complementary to a sequence of the UL 52 essential gene of HSV-1 (20). For the localization study, PS was labelled at the 5′ end with fluoresceine isothiocyanate (FITC) (Eurogentec, Seraing, Belgium). It was purified by 25% denaturing polyacrylamide gel electrophoresis (PAGE) (11). For the determination of the quantity of PS delivered to the skin, PS was labelled at the C8 position of the purine bases by hydrogen exchange with tritiated water (11), according to the method of Graham *et al.* (21). The

[1] Université Catholique de Louvain, Unité de Pharmacie Galénique, Avenue E. Mounier, 73 UCL 73.20, 1200 Brussels, Belgium.

[2] To whom correspondence should be addressed. (e-mail: preat@farg.ucl.ac.be)

0724-8741/98/1000-1596$15.00/0 © 1998 Plenum Publishing Corporation

specific activity of the ^{3}H-labelled PS was 0.11 mCi/μmoles. The purity of the ^{3}H-labelled PS was checked by PAGE.

In Vitro Model

The *in vitro* model was a polycarbonate vertical diffusion chamber made of 2 compartments separated by hairless rat skin, with epidermis facing the upper (donor) compartment. Full-thickness abdominal rat skin samples (Mutant Iops hairless rat, Iffa Credo, S^t Germain les Arbresles, France) were prepared by gently scraping off subcutaneous fat of freshly excised skin. Skin samples without stratum corneum (stripped skin) were prepared by tape-stripping the skin 9 times (Scotch Cristal, 602, Cergy Pontoise, France) before setting the diffusion cell. The skin area exposed to both solutions was 1 cm^2. Platinum pure electrodes (0.25 cm^2, Johnson Matthey, Brussels, Belgium) separated by 1 cm were used. The cathode was in the upper compartment while the anode was in the lower compartment. The upper compartment was filled with 0.5 ml of PS solution (3.3 μM PS in 0.04 M Hepes buffer, pH 7, with EDTA 1 mM, isotonized with 8% w/v sucrose). EDTA was added to avoid enzymatic degradation of the FITC-PS (18). The lower compartment contained 2.5 ml of 0.024 M phosphate buffer, pH 7.4 made isotonic with 4% w/v glucose. The lower compartment was maintained at 37°C and continuously stirred. No shift in pH due to pulsing was observed.

Topical Delivery of PS

PS was delivered to intact or stripped skin by electroporation or iontophoresis. The electric protocols were chosen to transfer equivalent amount of electric charges. Indeed, this parameter allows the control of the transport of PS upon application of high voltage pulses (11,12), but also determines the amount of drug delivered by iontophoresis (22). Given that the removal of the stratum corneum prior to pulsing has been shown to increase the concentration of PS in the target tissues by one order of magnitude (11), experiments were performed with both intact or stripped skin. Finally, as PS is transported in the skin viable tissues essentially during pulsing (12), it was not allowed to diffuse after the electric treatments. Results were compared with 21 min passive diffusion controls.

Iontophoresis (0.5 mA/cm^2) was applied during 21 min using a constant-current power supply. The total charge transferred (Q_{ionto}) was 0.63 C. It was calculated according to the equation $Q_{ionto} = i \cdot t$, where i is the current applied and t is the duration of the electric treatment.

The electroporation device (Easyject Plus®, Cell One, Herstal, Belgium) delivers exponentially-decaying (ED) capacitive discharge pulses, characterized by their initial voltage ($U_{electrodes}$) and their pulse time (τ). τ corresponds to the time required for the voltage to drop to 37% of its initial value. τ was measured by the electroporation device. This parameter depends on the resistance of the electric circuit (R_c, composed of two resistances in parallel: the shunt resistance (R_s) of Easyject plus and the apparent resistance of the diffusion chamber (R_{dc})) and the capacity of the electroporation device (C), following the equation. $\tau = R_c \times C$. The pulsing protocol used consisted in applying 5 pulses of 200 V, with $R_s = 201\ \Omega$ and C = 2.85 mF, resulting in pulses of $\tau = 494 \pm 13$ ms for intact skin, and $\tau = 457 \pm 14$ ms for stripped skin. Pulses were separated by 1 min. The pulses series are expressed as follows: 5 × (200 V − 494 ms) for intact skin and 5 × (200 V − 457 ms) for stripped skin. These pulses deliver PS at a therapeutic level (>1 μm) in the viable skin (11). Before electroporation, PS was allowed to diffuse passively in the skin during 17 min. Thereby, the total duration of contact between the PS solution and the skin was 21 min, as when iontophoresis was applied. The total charge transferred during pulsing (0.55 C and 0.51 C, for intact and stripped skin, respectively) was calculated according to Regnier *et al.* (11).

Quantification of the ON in the Stratum Corneum and in the Skin Layers

After topical delivery of PS, the skin was recovered from the diffusion chamber and was gently wiped clean. If unstripped, skin was pinned flat and was tape-stripped 10 times (Scotch Cristal, Cergy Pontoise, France) to remove the stratum corneum, and the area exposed to the donor solution was excised. The strips (when PS was delivered to intact skin) and the remaining skin tissues (which we called the viable skin, corresponding to the viable epidermis and dermis) were then lyophilized to remove the tritium label which might have exchanged with water. The dry samples were digested with NaOH, and counted for radioactivity (Beta Counter, Wallac 1410, LKB, Pharmacia). ON quantities, expressed as mean ± standard error of the mean (n = 3 to 8), were calculated from the total ^{3}H radioactivity in the stratum corneum or the viable skin and were compared by two way analysis of variance (Anova, $p < 0.05$). PS concentration in the skin viable tissues was calculated according to Regnier *et al.*(11).

PS Localization in the Skin

Immediately after topical delivery of the FITC-labelled PS by electroporation, iontophoresis or passive diffusion (see above), the skin samples were removed from the diffusion chamber, and gently wiped clean.

Standard Fluorescence Microscopy

To determine the permeation of the macromolecules into the skin tissues, the skin samples were snap frozen in isopentane cooled by liquid nitrogen and kept at −80°C before sectioning. Cryostat sections, 20 μm thick, were performed perpendicular to the skin surface. Sections were mounted without fixation with glycerol:water (9:1) with 0.002% 33258 Hoechst (W/V) for cell staining. Hoechst 33258 is a cell permeant, minor groove-binding DNA stain that fluoresces bright blue upon binding to DNA. The cross sections were viewed and photographed with a Leitz Orthoplan microscope equipped with Orthomat for microphotography. Sections were photographed using two different filters (λ_{exc} = 450–490 nm or 340–380 nm), to visualize FITC-PS or Hoechst 33258, respectively. All photographs were taken with 10× or 25× objectives and exposure time of 30–90 sec.

To view the transport regions (LTR) which were reported to be localized (11,13,23), the samples of skin were immediately placed on slides, with epidermis upwards. They were covered with coverslip glasses, and placed under the microscope. The LTRs were counted by screening the total skin surface (1 cm^2).

Three to five samples were counted and the mean number of LTRs was calculated. Skin was viewed and photographed under light of λ_{exc} = 450–490 nm to visualize FITC-PS, with a 40× lens and exposure time of 30–60 sec.

Laser Scanning Confocal Microscopy (LSCM)

LSCM was chosen to localize the ON in the epidermal cells as this technique allows localization of fluorescent molecules without shrinkage or distortion of the living tissue (24). The skin samples were directly placed in a sample holder (epidermis upwards) covered with coverslip glasses, and placed into the LSCM system. The confocal microscope system used was a BioRad MRC 1024 confocal unit equipped with an argon-krypton laser (excitation lines at 488 and 568 nm) and mounted on a Zeiss Axiovert 135M inverted microscope. The FITC-PS was detected using a BioRad filterblock, which selects the 488 nm laser line to illuminate the specimen, and transmits emitted light with a wave length in the range 522–535 nm. Images were obtained using a Zeiss Plan-Neofluar 40× oil immersion objective. Optical sectioning was performed parallel to the skin surface (xy planar optical section), at different focal planes (z = −2.5 to −55 μm), the z axis being perpendicular to the plane of the skin surface. The skin surface (z = 0) is defined (by the user) as the imaging plane of brightest fluorescence with a morphology characteristic of the stratum corneum surface (intact skin) or viable epidermis (stripped skin). All images were the average of 3–7 scans per image, and were obtained with the same optical aperture, filterblock, lens, black level and scan speed. Different laser intensities were used as function of the emission intensity.

To investigate the autofluorescence properties of the skin, samples were investigated with the confocal microscope in the absence of FITC-PS. The autofluorescence of rat skin was found to be very low with the confocal settings used in this study. To check whether the subcellular fluorescence observed after pulsing originated from FITC or FITC-PS, we delivered free FITC (3.3 μM in the same Hepes buffer) to stripped skin as a control.

RESULTS

PS was delivered *in vitro* to intact or stripped hairless rat skin by application of high-voltage electric pulses (5 × (200 V ~470 ms) or iontophoresis (0.5 mA/cm^2 during 21 min). Passive diffusions of 21 min were performed as controls.

Quantification of PS in the Skin

The amount of ON was measured both in the stratum corneum and the viable skin (see material and methods for details), the latter being potential target for antisense therapy.

Compared with the passive diffusion control, electroporation increased the topical delivery of the macromolecule by more than one order of magnitude. Electroporation was less efficient than iontophoresis to deliver PS in the viable tissues of intact skin, for approximately the same total charge transferred (Fig. 1A). The concentration of PS within the viable tissues was 0.4 μM after pulsing and 1.8 μM after iontophoresis. The quantities of PS retained in the stratum corneum after each of the electric treatments were not different ($p < 0.05$) (Fig. 1B). Both electric protocols delivered PS to the same extend to stripped skin (Fig. 2), allowing tissue concentrations of ON above 3 μM. After passive diffusion (21 min), the amount of PS found in the viable skin was one third of the quantities transported by iontophoresis or electroporation.

PS Localization in the Skin

The following experiments investigated the localization of FITC-PS, at the tissular level and cellular level, after delivery by electroporation or iontophoresis, keeping in mind that ON cellular uptake is required for an antisense effect. The localization of the oligomer in the skin tissues was performed with a FITC-labelled derivative of PS. Standard fluorescence microscopy was used to evaluate the permeation of PS within the skin at the tissue level and laser scanning confocal microscopy (LSCM) was used to ascertain PS distribution in the skin at the cellular level.

Localized Transport Regions (LTRs) of FITC-PS

The transport of FITC-PS in intact or stripped skin due to both pulsing or iontophoresis was found to be localized and often included an appendage for iontophoresis. For both intact or stripped skin, the LTRs (Localized Transport Regions) due to electroporation were of similar size, but approximately 5-fold more numerous than the LTRs due to iontophoresis (Table 1). After delivery of FITC-PS to intact skin by pulsing, however, the homogeneous staining of the skin surface with the fluorophore masked the LTRs, and we had to strip the skin before counting. The passive diffusion control showed, for intact skin, a very light fluorescence associated with dead corneocytes of the skin surface, and for stripped skin, a light fluorescence of the entire skin surface (data not shown).

Distribution of PS Within the Skin

To evaluate the depth of permeation of PS in the LTRs, the skin samples were snap frozen immediately after PS delivery and were cross sectioned. The slices were mounted with 33258 Hoechst for skin counterstaining and viewed at two wavelengths by standard fluorescence microscopy.

When the fluorescent macromolecule was delivered to intact skin by electroporation or by iontophoresis, it locally penetrated the entire thickness of the epidermis (Fig. 3). However, whereas FITC-PS was not transported deeper by electroporation (Fig. 3A), iontophoresis allowed it to reach the superficial layers of the dermis close to the hair follicles (Fig. 3B). The bright fluorescence of the stratum corneum after both electric protocols indicated an accumulation of PS in this layer (12). By passive diffusion, FITC-PS did not go beyond the stratum corneum (Fig. 3C).

After delivery of FITC-PS to stripped skin by electroporation or iontophoresis, the epidermis showed a fluorescence pattern similar to that observed with intact skin (Fig. 4). However, fluorescence was also recovered in the superficial layers of the dermis, where locally it penetrated deep (>200 μm) after both electric treatments. This local permeation of the fluorescence in the dermis was mainly associated with hair follicles for iontophoresis. The passive permeation of FITC-PS across stripped skin was restricted to the outermost layer of keratinocytes.

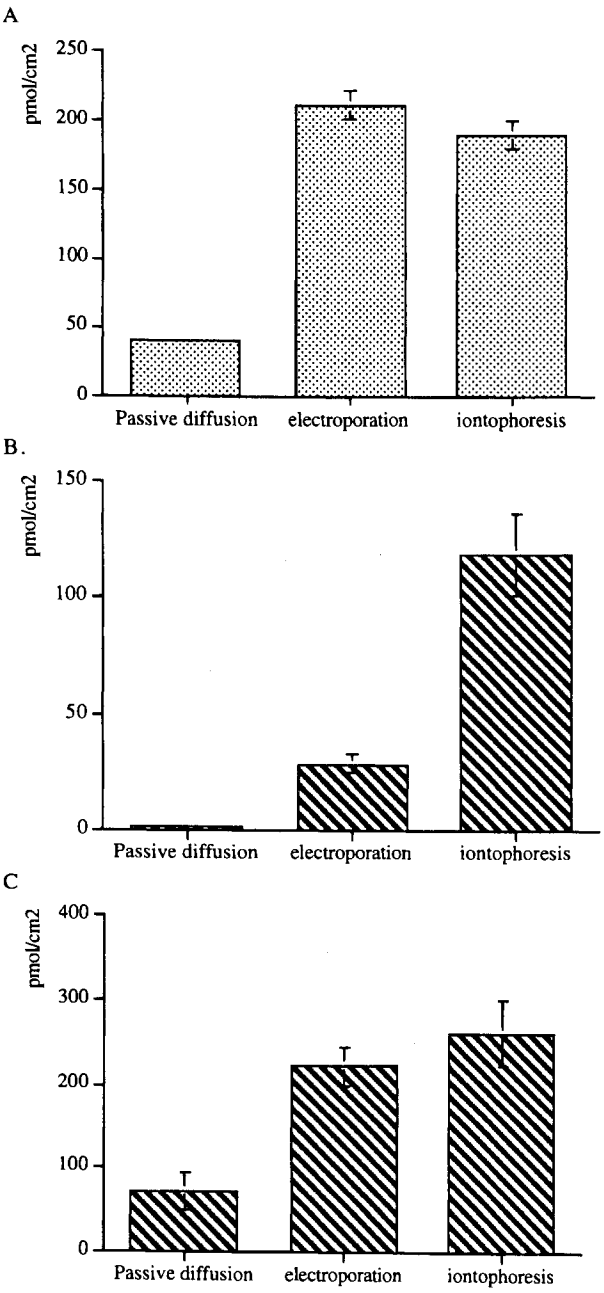

Fig. 1. Topical delivery of PS to intact skin: mean quantities of PS (pmol/cm^2) recovered in the skin viable tissues (A) or the stratum corneum (B) after 21 min passive diffusion, pulsing (5 × (200 V − 494 ms); Q = 0,55C), preceeded by 17 min passive diffusion (electroporation) or iontophoresis (0.5 mA/cm^{2-}-21 min; Q = 0,63C). (C) Topical delivery of PS to 10 times stripped skin: mean quantities of PS (pmol/cm^2) recovered in the viable skin after 21 min passive diffusion, pulsing (5 × (200 V − 457 ms); Q = 0,51C), preceeded by 17 min passive diffusion (electroporation) or iontophoresis (0.5 mA/cm^{2-}-21 min; Q = 0,63C). The total charge transferred (Q) is given for each electric protocol. Donor composition: ON 3.51 μM, EDTA 1 mM in 0.04 M Hepes buffer, pH 7, with sucrose 8% for isotony. n = 3–7.

Fine Localization of FITC-PS in the Epidermis by LSCM

LSCM was used to evaluate the distribution of FITC-PS at the cellular level in the viable epidermis, within the LTRs.

Immediately after electroporation of intact skin, FITC-PS was found between z = −15 and −55 μm (i.e., in the viable epidermis) in the nuclei of the keratinocytes (Fig. 4A), sometimes near brightly fluorescent hair follicles. In contrast, after iontophoresis, the fluorescent ON was never found within the keratinocytes. Paracellular pathways (Fig. 4B) were often associated with transfollicular pathways, FITC-PS being often detectable in the hair follicles below z = 80 μm. However, endocytosis of the FITC-PS but no nuclear localization was observed hours after iontophoresis (data not shown). By passive permeation, no fluorescence was found below z = −5 μm, the FITC-PS permeating only some corneocytes of the skin surface (data not shown).

Similar results were found when FITC-PS was delivered to stripped skin by either pulsing (Fig. 4C) or by iontophoresis (Fig. 4D). A nuclear staining of the keratinocytes in the LTRs was observed after electroporation. After passive permeation, the ON was rarely found below the first cell layer (data not shown).

As a control, FITC was also delivered by high-voltage pulsing, to ensure that the nuclear localization of the fluorescence was not due to free fluorescent label. Results showed that the fluorescence pattern due to free FITC or to FITC-PS was different: the fluorescence, due to free FITC was diffuse inside the keratinocytes without nuclear accumulation. Besides, the edges of the corneocytes were well marked (data not shown).

DISCUSSION

This report presents evidence for a fast ON uptake by the keratinocytes of freshly excised rat skin after electroporation. LSCM showed that FITC-PS accumulates in the nucleus of the viable keratinocytes a few minutes after pulsing. In contrast, iontophoresis, which delivers equivalent or higher amount of FITC-PS in the viable epidermis, did not lead to an uptake of the oligomer. Therefore, the internalization of FITC-PS after electroporation is very likely due to keratinocyte electropermeabilization.

Once introduced in the keratinocytes by electroporation, FITC-PS accumulated in the nucleus. This subcellular localization of an ON into keratinocytes is in agreement with other studies. Indeed, Chin *et al.* (25) reported the rapid i.e. within a few minutes, nuclear accumulation of ON, including phosphorothioates, after *in vitro* microinjection in keratinocytes. In contrast, hours of incubation of phosphorothioate ON (26) or phosphodiester ON (27) with keratinocytes in culture were needed to observe such nuclear accumulation. Besides, the introduction of phosphorothioate ON within other cell types (17) by electroporation led to a similar cellular trafficking of the oligomers.

The most important advantage of topical delivery of antisens ON by skin electroporation is the rapid cellular and nuclear uptake of antisense compounds by the keratinocytes. Consequently, skin electroporation: i) reduces ON exposure to the nucleases present in both extracellular fluids and endocytic compartments before hybridization of the ON with the target nucleic acid, ii) shortens the time of onset of the antisense effect, and iii) lowers the threshold ON concentration necessary to achieve such an effect. Bergan *et al.* (17) demonstrated that electroporation of cells in culture increases significantly the intracellular ON concentrations, while the expression of the

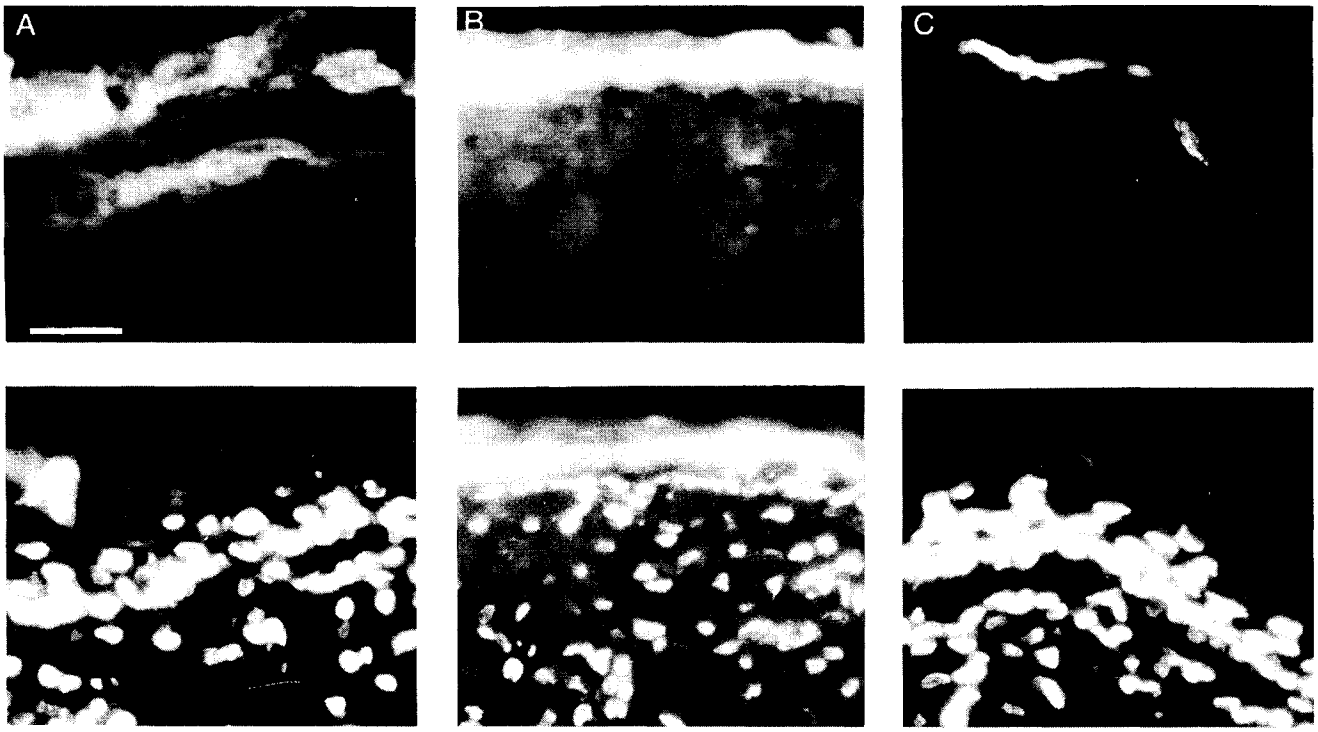

Fig. 2. Cross sections of intact skin showing the distribution of FITC-PS in the tissue after electroporation (5 × (200 V − 494 ms)) (A.1), iontophoresis (0.5 mA/cm^2 − 21 min) (B.1) or passive diffusion (21 min) (C.1). The sections were counterstained with 33258 Hoechst (A.2, B.2 and C.2, respectively). Hoechst 33258 fluoresces bright blue upon binding to DNA. Scale bar: 50 μm.

target gene was suppressed almost instantaneously, at much lower concentrations.

LSCM and standard fluorescence microscopy confirm that the molecular transport upon iontophoresis or medium voltage–long pulses is localized and often implies hair follicles for iontophoresis (10,23,24,28). Besides hair follicles, the pathways for FITC-PS transport were more paracellular during iontophoresis, as previously described for other molecules (24,28), and transcellular during electroporation (10,13,23). The random distribution and the size of the LTRs due to the two methods of delivery is equivalent, but the LTRs due to iontophoresis are less numerous. The LTRs observed on stripped skin are slightly more numerous than on intact skin. Within the LTRs, PS is found in the entire thickness of the epidermis, but iontophoresis allows the oligomer to permeate deeper intact skin, the first layers of the dermis being reached. This is probably linked to the deeper permeation of FITC-PS in the hair follicles by iontophoresis. When stripped skin was used, both methods allowed the ON to go beyond the epidermis.

Table 1. Size and Number of Localized Transport Regions (LTRs) Following Electroporation or Iontophoresis

		Number[a]	Size[a] (Diameter in mm)
Intact skin	Electroporation[c]	103[e]	0,2
	Iontophoresis[d]	21	0,4
Stripped skin[b]	Electroporation[c]	162	0,3
	Iontophoresis[d]	29	0,4

[a] Determined by standard fluorescence microscopy in perpendicular geometry.
[b] Skin was stripped 10 times before the electric treatment.
[c] 17 min passive diffusion followed by 5 × (200 V ~ 470 ms).
[d] 0.5 mA/cm^2 during 21 min.
[e] Counted after one stripping.

From a quantitative point of view, both iontophoresis and electroporation enhance significantly the delivery of PS in the skin. However, the comparison of the quantities of ON delivered makes sense only if the localization of the molecule at the cellular level is equivalent. We hypothetized that electroporation could be more efficient than iontophoresis to deliver ON in the viable epidermis because it has been reported that electroporation permeabilize both the stratum corneum and the epidermal cells. The localization of the ON after electroporation and iontophoresis confirms this hypothesis. Given the rapid internalization of PS in the keratinocytes, electroporation should thus be preferred to iontophoresis, even if iontophoresis is as or more efficient to deliver ON. Usually, with the same number of charges transported as basis of comparison, electroporation is more efficient than iontophoresis for transdermal delivery (29).

CONCLUSIONS

We showed that electroporation allows i) rapid delivery of ON in the epidermis, ii) delivery at a therapeutic level, and iii) fast ON uptake by the keratinocytes. Moreover, the quantities delivered can be controlled by the electric parameters of the

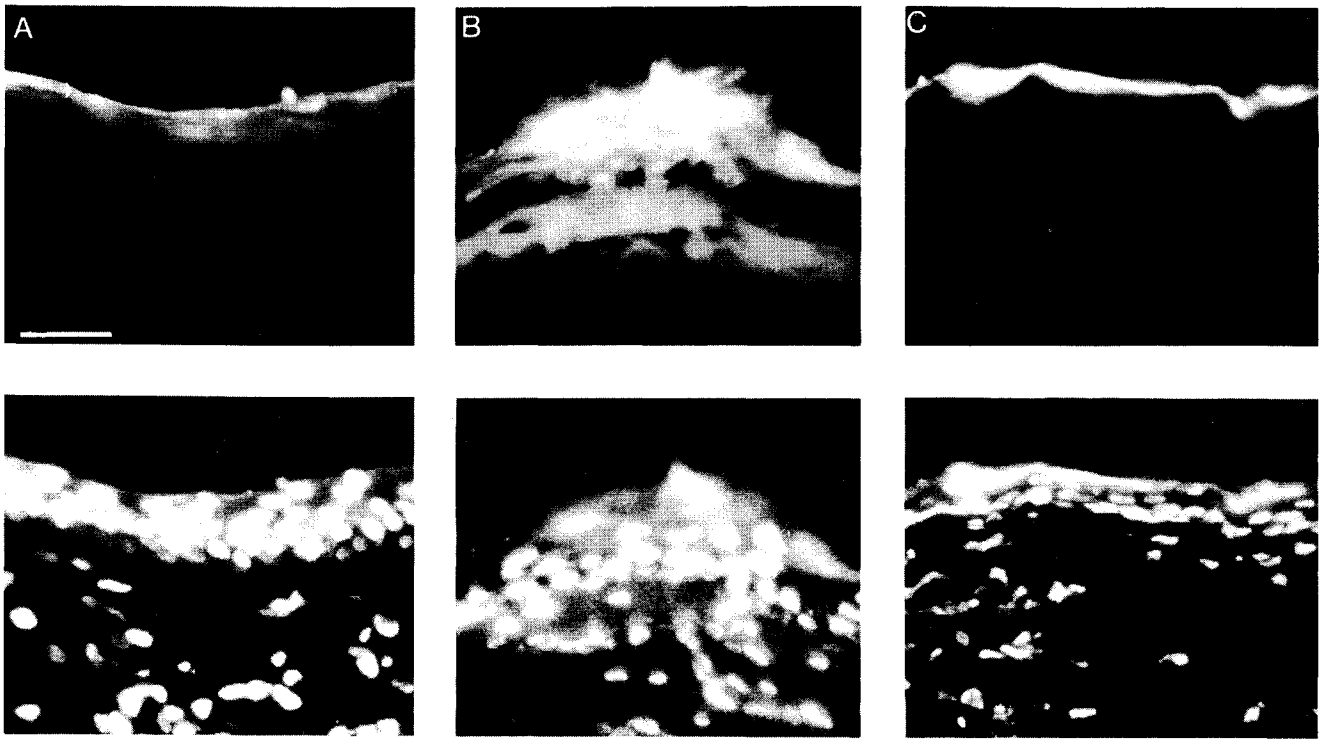

Fig. 3. Cross sections of stripped skin showing the distribution of FITC-PS in the tissue after electroporation (5 × (200 V − 457 ms)) (A.1), iontophoresis (0.5 mA/cm^2 − 21 min) (B.1) or passive diffusion (21 min) (C.1). The sections were counterstained with 33258 Hoechst (A.2, B.2 and C.2, respectively). 33258 Hoechst fluoresces bright blue upon binding to DNA. Scale bar: 50 μm.

pulses (i.e. the pulse voltage, pulse time and number of pulses), or the ON concentration in the donor compartment (11). The hypothesis that electroporation enhances both stratum corneum and keratinocyte permeability was confirmed. Hence, all the epidermal diseases that are confined to the epidermis or to the first layers of the dermis if the skin barrier is damaged, and for which the repression of the expression of a single protein may lead or contribute to the cure, are potential candidates to therapy by antisense ON delivered topically by electroporation.

ACKNOWLEDGMENTS

The authors thank 1) Cell one (Seraing, Belgium) for lending the electroporation device Easyject Plus®, 2) Eurogentec (Seraing Belgium) for giving the oligonucleotides, 3) Pr. P. Baudhuin and Pr. P. Courtoy for the use of CLSM and P. Van Der Smissen for his assistance with the CLSM (Laboratoire de Biologie Cellulaire, Institute of Molecular and Cellular Pathology (ICP), Brussels), 4) T. Le Doan (Laboratoire de Biochimie

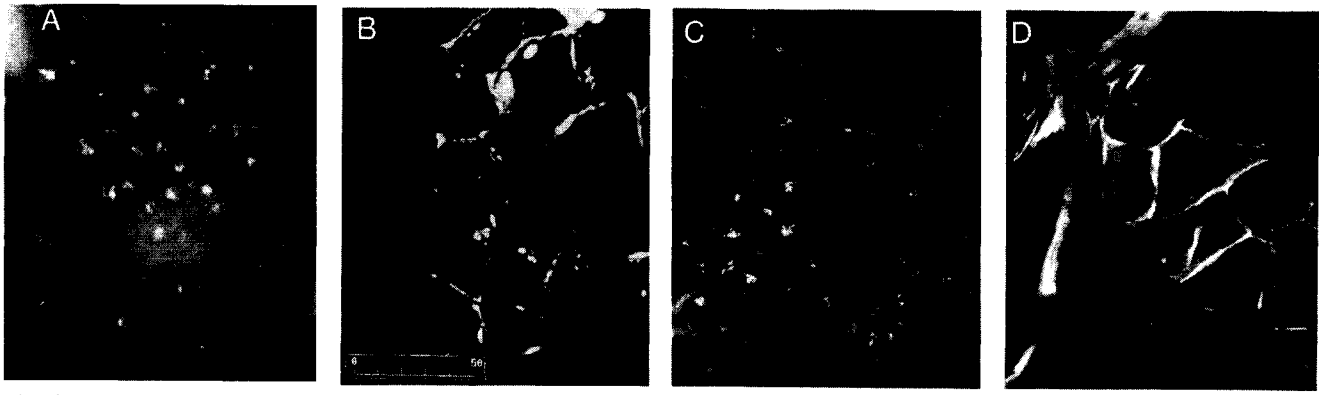

Fig. 4. xy-planar LSCM sections showing the distribution of FITC-PS in intact skin after electroporation (5 × (200 V − 494 ms)) (A) or iontophoresis (0.5 mA/cm^2 − 21 min) (B), or in stripped skin after electroporation (5 × (200 V − 457 ms)) (C) or iontophoresis (0.5 mA/cm^2 −21 min) (D). The images were acquired at depths 35 μm or 20 μm below the surface of intact or stripped skin, respectively, corresponding to a depth of approximatively 20 μm in the viable epidermis. Scale bar: × μm.

des Transports Cellulaires, Université de Paris XI, France) for helpful discussions, 5) H. Taper (Unité de Biochimie toxiciologique et cancérologique, Université catholique de Louvain) for the flouorescence microscope and helpful discussions, and 6) A. Tahiri (Laboratoire de Pharmacie Galénique, Université Catholique de Louvain, Brussels) and R. M. Dujardin for technical support. This work was supported by Fonds National de la Recherche Scientifique (FNRS, Belgium), by Région Wallone (Programme FIRST, Belgium) and by La Communauté Française de Belgique as part of C.G.R.I. - F.N.R.S. - C.N.R.S. cooperation programme. V. Préat is a senior research associate of F.N.R.S. The LSCM was financed by F.R.S.M. n° 9.4531.94F.

REFERENCES

1. Crooke and C. F. Bennett. Progress in antisense oligonucleotide therapeutic. *Annu. Rev. Pharmacol. Toxicol.* **36**:107–129 (1996).
2. F. Plenat. Animals models of antisense oligonucleotides: lessons for use in humans. *Mol. Med. Today.* **2**:250–257 (1996).
3. Tonkinson and C. A. Stein. Antisense oligonucleotides as clinical therapeutic agents. *Cancer Invest.* **14**:54–65 (1996).
4. Y. Rojanasakul. Antisens oligonucleotides therapeutics: drug delivery and targeting. *Adv. Drug Del. Rev.* **18**:115–131 (1996).
5. H. W. Nolen III, P. Catz, and D. R. Friend. Percutaneous penetration of methyl phosphonate antisense oligonucleotides. *Int. J. Pharm.* **107**:169–177 (1994).
6. J. Weaver. Electroporation theory. Concepts and mechanisms. *Methods. Mol. Biol.* **47**:1–26 (1995).
7. M. R. Prausnitz, U. Pliquett, R. Langer, and J. C. Weaver. Rapid temporal control of transdermal drug delivery by electroporation. *Pharm. Res.* **11**:1834–1837 (1994).
8. R. Vanbever and V. Préat. Factors affecting transdermal delivery of metoprolol by electroporation. *Bioelectrochem. Bioenerget.* **38**:223–228 (1995).
9. R. Vanbever, E. LeBoulangé, and V. Préat. Transdermal drug delivery of fentanyl by electroporation I. Influence of electrical factors. *Pharm. Res.* **13**:557–563 (1996).
10. R. Vanbever. Skin electroporation for transdermal drug delivery. PhD. Thesis. Université Catholique de Louvain. Brussels Belgium. 1997.
11. V. Regnier, T. Le Doan, and V. Préat. Parameters controlling topical delivery of oligonucleotides by electroporation. *J. Drug Target.* in press.
12. V. Regnier and V. Préat. Mechanisms of a phosphorothioate oligonucleotide delivery by skin electroporation. *Int. J. Pharm.*, in press.
13. T. E. Zewert, U. F. Pliquett, R. Langer, and J. C. Weaver. Transdermal transport of DNA antisense oligonucleotides by electroporation. *Biochem. Biophys. Res. Commun.* **212**:286–292 (1995).
14. J. Belehradek Jr, S. Orlowski, L. H. Ramirez, G. Pron, B. Poddevin, and L. M. Mir. Electropermeabilization of cells in tissues assessed by the qualitative and quantitative/ electroloading of bleomycin. *Biochim. Biophys. Acta.* **1190**:155–163 (1994).
15. A. V. Titomirov, S. Sukharev, and E. Kistanova. In vivo electroporation and stable transformation of skin cells of newborn mice by plasmid DNA. *Biochim. Biophys. Acta.* **1088**:131–134 (1991)
16. L. Zhang, L. Li, G. A. Hoffmann, and R. M. Hoffman. Depth-targeted efficient gene delivery and expression in the skin by pulsed electric fields: an approach to gene therapy of skin ageing and other diseases. *Biochem. Biophys. Res. Commun.* **220**:633–636 (1996).
17. R. Bergan, Y. Connell, B. Fahmy, and L. Neckers. Electroporation enhances c-myc antisense oligodeoxynucleotide efficacy. *Nucleic. Acids. Res.* **21**:3567–3573 (1993).
18. K. R. Oldenburgh, K. TVo, G. A. Smith, and H. E. Selick. Iontophoretic delivery of oligonucleotides across full thickness hairless mouse skin. *J. Pharm. Sci.* **84**:915–921 (1995).
19. R. Brand and P. Iversen. Iontophoretic delivery of a telomeric oligonucleotide. *Pharm. Res.* **13**:851–854 (1996).
20. B. Roizman. Inhibition of Herpesviridae infection by antisense oligonucleotides. PCT WO 92/03051 (1992).
21. M. J. Graham, S. M. Freier, R. M. Crooke, D. J. Eckler, R. N. Maslova, and E. A. Lesnik. Tritium labelling of antisense oligonucleotides by exchange with tritiated water. *Nucleic Acids. Res.* **21**:3737–3743 (1993).
22. P. Green. Iontophoretic delivery of peptide drugs. *J. Control. Rel.* **41**:33–48 (1996).
23. M. Prausnitz, Gimm J., Guy R. H., Langer R., Weaver J., and C. Cullander. Imaging of transient pathways across human, stratum corneum during high voltage and low voltage electrical exposures. *J. Pharm. Sci.* **85**:1363–1370 (1996)
24. C. Cullander and R. H. Guy. Visualization of iontophoretic pathways with confocal microscopy and the vibrating probe electrode. *Solid States Ion.* **53–56**:197–206 (1992).
25. D. J. Chin, G. A. Green, G. Zon, F. C. Szoka Jr., and R. M. Straubinger. Rapid nuclear accumulation of injected oligodeoxyribonucleotides. *New Biol.* **12**:1091–1100 (1990).
26. C. Giachetti and D. J. Chin. Increased oligonucleotide permeability in keratinocytes of artificial skin correlates with differentiation and altered membrane function. *J. Invest Dermatol.* **106**:412–418 (1996).
27. S. B. Noonberg, M. R. Garovoy, and C. A. Hunt. Characteristics of oligonucleotide uptake in human keratinocyte cultures. *J. Invest. Dermatol.* **101**:727–731 (1993).
28. N. A. Monteiro-Rivière, A. O. Inman, and J. E. Rivière. Identification of the pathways of iontophoretic delivery: light and ultrastructural studies using mercuric chloride in pigs. *Pharm. Res.* **11**:251–256 (1994).
29. V. Préat, R. Vanbever, A. Jadoul, and V. Regnier. D. Duchêne et al. (Eds), Electrically enhanced transdermal drug delivery: iontophoresis vs electroporation. in *Iontophoresis*, Eds D. Duchêne et al., Editions de la santé, Paris, in press.